DYNAMIC DEFORMATIONS AND STRESSES OF BEAMS CONNECTED BY DAMPING ELEMENT

Ladislav Půst*

Dynamic properties of two similar, parallel, one-sided clamped beams connected by a damping element on their free ends are analytically and numerically investigated. A harmonic motion excites the end of one of these beams. The main attention is given to the ascertaining of response curves deflection shapes of beams and their stresses in roots at different orientations and levels of damping force.

Keywords: *beam vibration, damping, modes of forced vibration, stress in roots*

1. Introduction

Plenty of publications were devoted to the problem of beam oscillations i.e. [1–6] both in Czech and in world literature. In spite of this, some special cases of beam systems were not yet analyzed, particularly those connected with the new machine structures or machine elements. For ascertaining of dynamic properties and damping possibilities of turbine blades [7, 8, 10] a simplified model consisting of two parallel beams with constant cross-sections, connected at their ends by a dry friction element was investigated. This friction area lies in the vertical symmetry plane of the two-beams system. Analyses verified by experimental measurements proved very good efficiency of this damping principle, as well as its influence on response curves and shift of resonance peaks. The forms of beams deformations at different frequencies of excitation and at different positions of damping contact area were not yet studied.
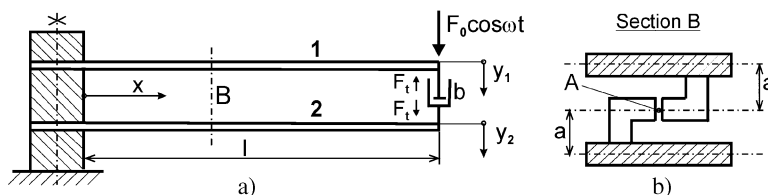

Fig.1: Schema of investigated two-beams system

The presented contribution is oriented on this special problem, which it is very important from the point of view of distribution of stress and strain in beams at given conditions. We will concentrate our attention on the influence of eccentricity of contact area position from the neutral axis of beams, because this eccentricity influences considerably the form of beam deformation.

In the technical applications the damping in contact area is realized by dry friction, described in its simplified form by strongly nonlinear Coulomb Law. For two-dimensional

---

* Ing. L. Půst, DrSc., Institute of Thermomechanics AS CR, v.v.i., Dolejškova 5, 18200 Praha 8

relative motion in contact area is due to the nonlinearity the mathematical expression very complicated and not suitable for general analysis. Therefore we will apply the first approximation solution, which enables us to describe friction behavior by means of equivalent linearized coefficient of damping, with which the solution and its resultants will be obtained in a more compact form.

2. Investigated system

Schema of first case of investigated system is in Fig. 1, where the damping element at bending oscillations of beams 1 and 2 acts only in vertical direction. This model corresponds to real system only if the ends of damping element are connected with the ends of beams by means of revolving joints or if the length a of eccentricity of damping area is zero.

If these eccentricities are of length a and are rectangularly fixed to the beam ends, the relative motion in damping contact is given by two-dimensional displacements x, y of both areas (see Fig. 2a) and damping forces must be modeled by schema shown in Fig. 2b. Centers of both friction areas move relatively both in vertical direction y_{rel}, and, due to the inclinations of arms, also in horizontal direction x_{rel}.
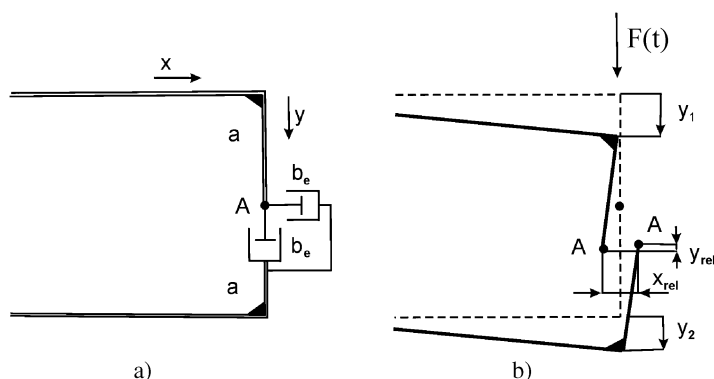

Fig.2: Two-dimensional displacement with components
x_{rel}, y_{rel} in damping contact area

Due to the very small ratio of length of arm a to free length l of beams, the mass and compliance of arm a can be neglected.

3. Equations of system motion

Motion equations of lateral oscillations of slender prismatic beams at neglecting influence of rotary inertia and shearing force are

$$E\,J\,\frac{\partial^4 y_i}{\partial x^4} + \rho\,S\,\frac{\partial^2 y_i}{\partial t^2} = 0\,,\qquad i = 1, 2\,. \tag{1}$$

According to Fourier method, the periodic solution of equation (1) can be written as a product of function of length x and of function of time t [1–6]:

$$y_i = X_i(x)\,T_i(t)\,,\qquad i = 1, 2\,. \tag{2}$$

This enables easy separation of both functions. After setting (2) into motion equations (1) these can be disconnected into two pairs of ordinary differential equations

$$\frac{\mathrm{d}^2 T_i}{\mathrm{d}t^2} + \omega^2\, T_i = 0 \;, \qquad \frac{\mathrm{d}^4 X_i}{\mathrm{d}x^4} - k^4\, X_i = 0 \;, \qquad i = 1, 2 \;, \tag{3}$$

where

$$k^4 = \frac{\rho\, S\, \omega^2}{E\, J} \;. \tag{4}$$

Unknown constant k (or ω) must be ascertained from the boundary conditions. For left sides of both beams clamped at their ends they are

$$x = 0 \;, \qquad y_i(0, t) = 0 \;, \qquad \frac{\partial y_i}{\partial x}(0, t) = 0 \;, \qquad i = 1, 2 \;. \tag{5a}$$

A prescribed motion $x_0\, \cos(\omega\, t)$ deflects the right end of upper beam harmonically at constant amplitude x_0. On this end acts also vertical component F_{ty} of damping force and moment from the horizontal component F_{tx} of damping force acting in friction area. The boundary conditions for the upper beam ($i = 1$) are

$$y_1(l, t) = x_0\, \cos(\omega\, t) \;, \qquad -E\, J\, \frac{\partial^2 y_1(l, t)}{\partial x^2} = a\, F_{\mathrm{tx}} \;, \qquad x = l \;. \tag{5b}$$
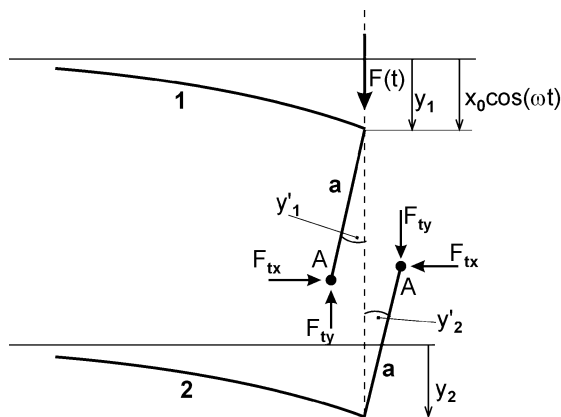

Fig.3: *Components F_{tx}, F_{ty} of damping force in friction area*

Forces in the friction area are drawn in Fig. 3. Damping forces at oscillations are modeled by means of equivalent coefficient of damping [1] ascertained from the equivalence of lost energy due to the dry friction and viscose equivalent linear damping at the same amplitude and frequency :

$$b_{\mathrm{e}} = \frac{4\, F_{\mathrm{t}}}{\pi\, a_{\mathrm{v}}\, \omega} \;.$$

Components of damping force F_{ty} and F_{tx} are proportional to the components of relative velocity of point A i.e. velocities

$$\dot{y}_{\mathrm{rel}} = \dot{y}_1 - \dot{y}_2 \;, \qquad \dot{x}_{\mathrm{rel}} = a\, (\dot{y}'_1 + \dot{y}'_2) \;. \tag{6}$$

Vertical and horizontal damping force components are

$$F_{\mathrm{ty}} = b_{\mathrm{e}}\,(\dot{y}_1 - \dot{y}_2) \quad \text{and} \quad F_{\mathrm{tx}} = b_{\mathrm{e}}\,a\,(\dot{y}'_1 + \dot{y}'_2)\ . \tag{7}$$

As bending of arms with small length a is neglected, the boundary conditions of the right end $(x = l)$ of upper beam $(i = 1)$ are

$$y_1(l,t) = x_0\,\cos(\omega\,t)\ , \qquad -E\,J\,\frac{\partial^2 y_1(l,t)}{\partial x^2} = a^2\,b_{\mathrm{e}}\left[\frac{\partial^2 y_1(l,t)}{\partial x\,\partial t} + \frac{\partial^2 y_2(l,t)}{\partial x\,\partial t}\right] \tag{8a}$$

and of bottom beam $(i = 2)$ are

$$\begin{aligned}
-E\,J\,y'''_2 &= b_e\,(\dot{y}_1 - \dot{y}_2)\ , \\
-E\,J\,y''_2 &= F_{\mathrm{tx}}\,a = b_{\mathrm{e}}\,a^2\,(\dot{y}'_1 + \dot{y}'_2)\ .
\end{aligned} \tag{8b}$$

In spite of different motions in directions x and y the same equivalent linear damping b_{e} is used in equations (6)–(8), because it depends on common amplitude $a_{\mathrm{v}} = \sqrt{x_{\mathrm{rel}}^2 + y_{\mathrm{rel}}^2}$, where x_{rel}, y_{rel} are relative displacements in contact point A.

4. Equations of motion and their solution

First of all we will find the periodic particular solution of equation (1) in the simple form, which is very often used in literature on beams vibrations e.g. [1–6, 9]:

$$T(t) = A_i\,\cos(\omega\,t) + B_i\,\sin(\omega\,t)\ , \tag{9}$$

$$Y(x) = C_i\,\cos(k\,x) + D_i\,\sin(k\,x) + E_i\,\cosh(k\,x) + F_i\,\sinh(k\,x)\ , \qquad i = 1, 2 \tag{9a}$$

with twelve integral constants, but due to the solution (2) in the form of product, two of them can be select arbitrary, e.g. $A_i = 1$:

$$T_i(t) = \cos(\omega\,t) + B_i\,\sin(\omega\,t)\ . \tag{9b}$$

Boundary conditions of clamped beams on left end (see eq. 5a) are fulfilled if

$$C_i = -E_i\ , \qquad D_i = -F_i\ , \qquad i = 1, 2 \tag{10}$$

and the curves of deflection are given by

$$Y_i(x) = C_i\,[\cos(k\,x) - \cosh(k\,x)] + D_i\,[\sin(k\,x) - \sinh(k\,x)]\ , \qquad i = 1, 2\ . \tag{11}$$

Vibrations of two-beams system are then described of equations (9b) and (11) containing six free constants: B_1, C_1, D_1, B_2, C_2, D_2. Because the expressions for motions $y_1(l,t)$ and $y_2(l,t)$ contain sinus and cosines components, the fulfilling of four boundary conditions (8a) and (8b) requires fulfilling of eight algebraic equations. It is evident that six free constants B_1, C_1, D_1, B_2, C_2, D_2 do not suffice and therefore the solution (2) in the form of one product does not describe the motion of two-beams system with eccentric friction area.

Influence of horizontal damping forces in equations (8a,b) must be expressed by another, complicated selection of periodic solution e.g. in the form

$$y_i(x,t) = Y_{i1}(x)\,T_{i1}(t) + Y_{i2}(x)\,T_{i2}(t)\ , \qquad i = 1, 2\ , \tag{12}$$

where the deformation functions $Y_{ij}(x)$ fulfill the conditions of rigid fixing on the left side (5a) and the build-up functions $y_i(l,t)$ fulfill the boundary conditions (8a,b). The simplest form with 8 free constants is

$$
\begin{aligned}
y_i(x,t) &= [\cosh(k\,x) - \cos(k\,x)]\,[A_i\,\cos(\omega\,t) + B_i\,\sin(\omega\,t)] + \\
&\quad + [\sinh(k\,x) - \sin(k\,x)]\,[C_i\,\cos(\omega\,t) + D_i\,\sin(\omega\,t)] = \\
&= \tilde{U}(k\,x)\,[A_i\,\cos(\omega\,t) + B_i\,\sin(\omega\,t)] + \\
&\quad + \tilde{V}(k\,x)\,[C_i\,\cos(\omega\,t) + D_i\,\sin(\omega\,t)]\,, \qquad\qquad i = 1,2\,.
\end{aligned}
\tag{13}
$$

After introducing notation

$$
\begin{aligned}
\tilde{U}(k\,x) &= \cosh(k\,x) - \cos(k\,x)\,, & \tilde{V}(k\,x) &= \sinh(k\,x) - \sin(k\,x)\,, \\
\tilde{S}(k\,x) &= \cosh(k\,x) + \cos(k\,x)\,, & \tilde{T}(k\,x) &= \sinh(k\,x) + \sin(k\,x)\,,
\end{aligned}
\tag{14}
$$

the lateral deformations of beams and their derivates are

$$
\begin{aligned}
y_i(x,t) &= \tilde{U}(k\,x)\,[A_i\,\cos(\omega\,t) + B_i\,\sin(\omega\,t)] + \\
&\quad + \tilde{V}(k\,x)\,[C_i\,\cos(\omega\,t) + D_i\,\sin(\omega\,t)]\,, \\
y_i'(x,t) &= k\,\tilde{T}(k\,x)\,[A_i\,\cos(\omega\,t) + B_i\,\sin(\omega\,t)] + \\
&\quad + k\,\tilde{U}(k\,x)\,[C_i\,\cos(\omega\,t) + D_i\,\sin(\omega\,t)]\,, \\
y_i''(x,t) &= k^2\,\tilde{S}(k\,x)\,[A_i\,\cos(\omega\,t) + B_i\,\sin(\omega\,t)] + \\
&\quad + k^2\,\tilde{T}(k\,x)\,[C_i\,\cos(\omega\,t) + D_i\,\sin(\omega\,t)]\,, \\
y_i'''(x,t) &= k^3\,\tilde{V}(k\,x)\,[A_i\,\cos(\omega\,t) + B_i\,\sin(\omega\,t)] + \\
&\quad + k^3\,\tilde{S}(k\,x)\,[C_i\,\cos(\omega\,t) + D_i\,\sin(\omega\,t)]\,, \\
\dot{y}_i(x,t) &= \omega\,\tilde{U}(k\,x)\,[-A_i\,\cos(\omega\,t) + B_i\,\sin(\omega\,t)] + \\
&\quad + \omega\,\tilde{V}(k\,x)\,[-C_i\,\cos(\omega\,t) + D_i\,\sin(\omega\,t)]\,, \\
\dot{y}_i'(x,t) &= \omega\,k\,\tilde{T}(k\,x)\,[-A_i\,\cos(\omega\,t) + B_i\,\sin(\omega\,t)] + \\
&\quad + \omega\,k\,\tilde{U}(k\,x)\,[-C_i\,\cos(\omega\,t) + D_i\,\sin(\omega\,t)]\,.
\end{aligned}
\tag{15}
$$

Setting $x = l$ into (15) and using these expressions into boundary conditions (8a,b), we get a set of four algebraic equations each with coefficients multiplied by $\sin(\omega\,t)$ and $\cos(\omega\,t)$. These coefficients present 8 algebraic equations with 8 unknown values A_i, B_i, C_i, D_i, $i = 1,2$. Let us introduce for simplicity following dimensionless parameters

$$
\kappa = k\,l\,, \qquad \varepsilon = \frac{a^2}{l^2}\,, \qquad \beta = \frac{b_{\mathrm{e}}\,l}{\sqrt{E\,J\,\rho\,S}}\,.
\tag{16}
$$

This procedure gives a set of 8 algebraic equations, linear in $A_1, \ldots, D_2$:

$$
\begin{aligned}
\tilde{U}\,A_1 + \tilde{V}\,C_1 &= x_0\,, \\
\tilde{U}\,B_1 + \tilde{V}\,D_1 &= 0\,, \\
\tilde{S}\,A_1 + \tilde{T}\,C_1 + \alpha\,\beta\,\kappa\,(\tilde{T}\,B_1 + \tilde{U}\,D_1 + \tilde{T}\,B_2 + \tilde{U}\,D_2) &= 0\,, \\
\tilde{S}\,B_1 + \tilde{T}\,D_1 - \alpha\,\beta\,\kappa\,(\tilde{T}\,A_1 + \tilde{U}\,C_1 + \tilde{T}\,A_2 + \tilde{U}\,C_2) &= 0\,, \\
\beta\,(\tilde{U}\,B_1 + \tilde{V}\,D_1 - \tilde{U}\,B_2 - \tilde{V}\,D_2) + \kappa\,(\tilde{V}\,A_2 + \tilde{S}\,C_2) &= 0\,, \\
\beta\,(-\tilde{U}\,A_1 - \tilde{V}\,C_1 + \tilde{U}\,A_2 + \tilde{V}\,C_2) + \kappa\,(\tilde{V}\,B_2 + \tilde{S}\,D_2) &= 0\,, \\
\tilde{S}\,A_2 + \tilde{T}\,C_2 + \alpha\,\beta\,\kappa\,(\tilde{T}\,B_1 + \tilde{U}\,D_1 + \tilde{T}\,B_2 + \tilde{U}\,D_2) &= 0\,, \\
\tilde{S}\,B_2 + \tilde{T}\,D_2 - \alpha\,\beta\,\kappa\,(\tilde{T}\,A_1 + \tilde{U}\,C_1 + \tilde{T}\,A_2 + \tilde{U}\,C_2) &= 0\,,
\end{aligned}
\tag{17}
$$

where shorter symbols $\tilde{U}, \ldots, \tilde{T}$ were used instead of $\tilde{U}(k\,l), \ldots, \tilde{T}(k\,l)$. For each value $\kappa = k\,l$ in the selected range $k\,l = 1.5$–2.5, which covers the frequency range of first resonance zone of a cantilever ($y''(l, t) = 0$) and of a beam with suppression of right-end-rotation ($y'(l, t) = 0$ – see Fig. 4), the values $A_1, \ldots, D_2$ can be single-valued calculated.
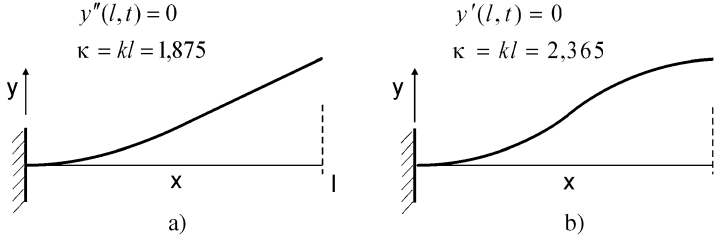

Fig.4: *Two limit forms of cantilever beam deflection*

By means of these determined values we are able to calculate amplitudes of right ends of both beams

$$a_i(k\,l) = \sqrt{\left[\tilde{U}(k\,l)\,A_i + \tilde{V}(k\,l)\,C_i\right]^2 + \left[\tilde{U}(k\,l)\,B_i + \tilde{V}(k\,l)\,D_i\right]^2}\,, \qquad i = 1, 2\,. \qquad (18)$$

As for upper beam is the end-amplitude prescribed and ascertained to value x_0, the amplitude of the second, bottom beam varies with variation of frequency parameter $k\,l$, or variation of excitation frequency $\omega = (k\,l)^2/l^2\,\sqrt{E\,J/(\rho\,S)}$. Example of these response curves for $a/l = 0.2$ and dimensionless damping $\beta = 0.05$; 0.25; 1.25; 6.25; 31.25 in contact area are in Fig. 5.

It is evident that amplitude of bottom beam increases with greater damping. Resonance peak gets closer to the amplitude $a_1 = x_0$ of right end of upper beam, but the resonance frequency increases as well.
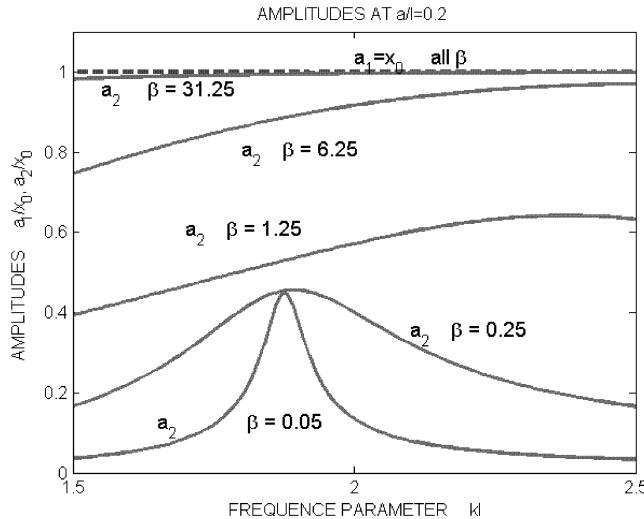

Fig.5: *Response curves of ends of upper (a1) and bottom (a2) beams*

The knowledge of coefficients $A_1, \ldots, D_2$ enable to ascertain also exciting force, which has to be used for ensuring the constant amplitude x_0 of right end motion for all values of frequency parameter $k\,l = 1.5\text{--}2.5$.

From the equilibrium of vertical forces acting on the upper beam end

$$-E\,J\,y_1'''(l,t) = F(t) - b_{\mathrm{e}}\,[\dot{y}_1(l,t) - \dot{y}_2(l,t)] \tag{19}$$

we get after introducing expressions for y_1, y_2 and $F(t) = F_0\,\cos(\omega\,t + \psi)$:

$$F_0\,\cos(\omega\,t + \psi) = \left\{-E\,J\,k^3\left(\tilde{V}\,A_1 + \tilde{S}\,C_1\right) + b_{\mathrm{e}}\,\omega\left[\tilde{U}\,(B_1 - B_2) + \tilde{V}\,(D_1 - D_2)\right]\right\}\cos(\omega\,t) +$$
$$+ \left\{-E\,J\,k^3\left(\tilde{V}\,B_1 + \tilde{S}\,D_1\right) + b_{\mathrm{e}}\,\omega\left[\tilde{U}\,(A_1 - A_2) + \tilde{V}\,(C_1 - C_2)\right]\right\}\sin(\omega\,t)\ .$$

Force amplitude F_0 in the dimensionless form is

$$\frac{F_0\,l^2}{E\,J} = (k\,l)^2\,\frac{x_0}{l}\left[\frac{\left\{-k\,l\left(\tilde{V}\,A_1 + \tilde{S}\,C_1\right) + \beta\left[\tilde{U}\,(B_1 - B_2) + \tilde{V}\,(D_1 - D_2)\right]\right\}^2}{x_0^2} +\right.$$
$$\left. + \frac{\left\{-k\,l\left(\tilde{V}\,B_1 + \tilde{S}\,D_1\right) + \beta\left[\tilde{U}\,(A_1 - A_2) + \tilde{V}\,(C_1 - C_2)\right]\right\}^2}{x_0^2}\right]^{\frac{1}{2}}\ . \tag{20}$$
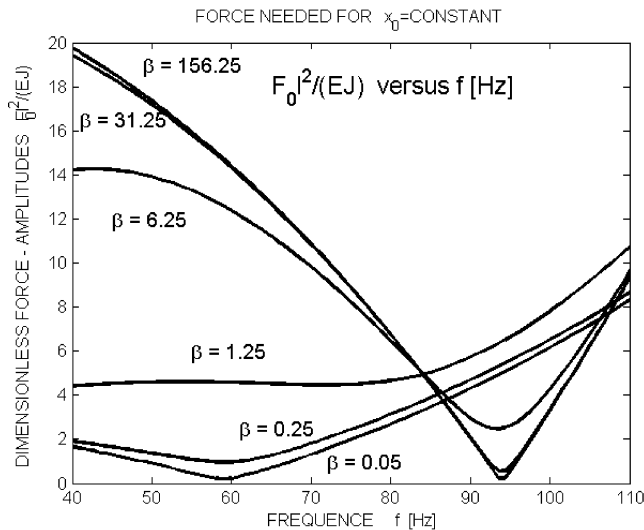

Fig.6: Variation of dimensionless force at constant amplitude $x_0/l = 0.001$

For $x_0/l = 0.001$ and $\beta = 0.05\text{--}156.25$ are the force – frequency curves plotted in Fig. 6. It is seen, that the amplitude of force, needed for sustaining the constant amplitude x_0 of displacement in the whole interval of frequency

$$f = \frac{\omega}{2\pi} = \frac{(k\,l)^2}{2\pi\,l^2}\,\sqrt{\frac{E\,J}{\rho\,S}} = 38\text{--}115\,\mathrm{Hz}\ , \qquad k\,l = 1.5\text{--}2.5$$

varies according to the damping β in contact area. For very low damping lies minimum of necessary force at $f = 58$ Hz. This minimum shifts to higher frequency at rising damping and reaches again its minimum value at very high damping $\beta > 30$ near frequency $f = 93$ Hz.

On the contrary, if the force F_0 is constant during the entire frequency range, then the amplitude of upper beam end oscillates with variable amplitude x_0/l, which can be calculated as inverse function of (20). These response curves are shown in Fig. 7. Two high resonance peaks – at $f = 58$ Hz for small damping and at $f = 93$ Hz for strong damping – are expressive.

These resonances differ not only by frequencies but also by the deflection forms of beams.
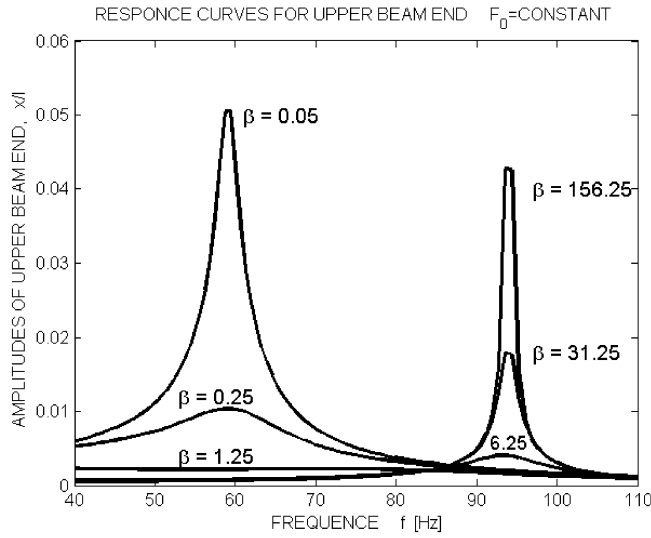

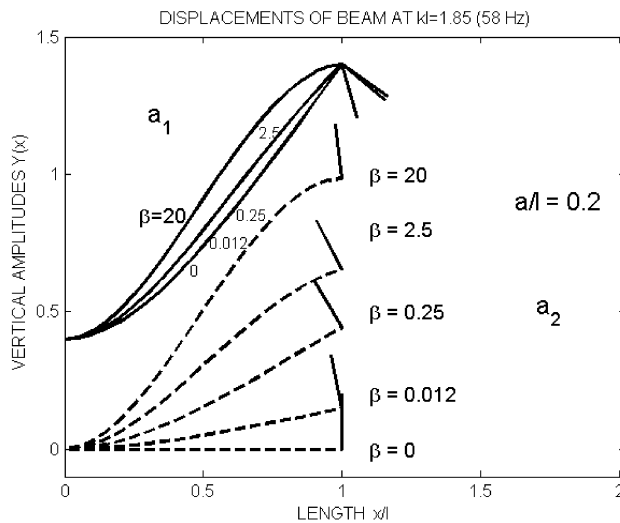Fig.7: *Variation of upper-beam-end amplitude at $F_0 = constant$*

Fig.8: *Variation of beams vibration modes $Y_i(x)$ with increasing dimensionless damp-ing β at constant amplitude $a_1/x_0 = 1$ of upper beam at $k\,l = 1.85$*

5. Modes of vibrations

Because the beams are pure elastic bodies, without any damping, their deformation – forced vibrations modes – are plane curves, which vary with excitation frequency and with the damping in end conditions. This mode-variation is best seen near the resonance frequencies $f = 58$ and $93\,\text{Hz}$ (see Fig. 7).

Mode of vibration can be deduced from equation (13) after elimination time t.

$$Y_i(x) = \sqrt{\left[\tilde{U}(k\,x)\,A_i + \tilde{V}(k\,x)\,C_i\right]^2 + \left[\tilde{U}(k\,x)\,B_i + \tilde{V}(k\,x)\,D_i\right]^2}\,, \qquad i = 1, 2\,. \tag{21}$$

Values $A_i, \ldots, D_i$ calculated from system of equations (17) depend on parameters κ, a/l, β. For constant $\kappa = k{,}l = 1.85$ ($f = 58\,\text{Hz}$) and $a/l = 0.2$ and for five values of dimensionless damping $\beta = 0$–20 are deformations of both beams shown in Fig. 8.

Positions of perpendicular branches with friction areas on their ends are shown as well on this Figure. All curves are drawn for the same constant amplitudes $Y_1(l) = 1$ of the upper beam end. Without damping ($\beta = 0$) moves only the upper beam and its deformation is ascertained by $Y''(l) = 0$ (see Fig. 4a). Increasing damping ($\beta = 0.012$–20) causes motion of bottom beam (dashed lines, $i = 2$), and increase of damping forces between the upper and bottom beams. Horizontal force component bends the free ends of both beams and deflection curves approximate the limit cases (Fig. 4b) for $y'(l, t) = 0$.

Similar modes of vibrations are drawn in Fig. 9 for second resonance ($k\,l = 2.36$, $f = 93\,\text{Hz}$). Increasing damping coefficient β changes again the modes of vibrations from the form shown in Fig. 4a to Fig. 4b. Due to this variation of deflection form, the both friction areas (ends of perpendicular branches) get nearer and the energy lost by damping decreases. For $\beta = 50$ are both branches almost connected, lost energy is near to minimum and the system is very weakly damped. At given resonance frequency are amplitudes of both beams very high – see Fig. 7 – or the force amplitude at constant kinematics excitation $x_0 = \text{const}$ is very low – see Fig. 6.
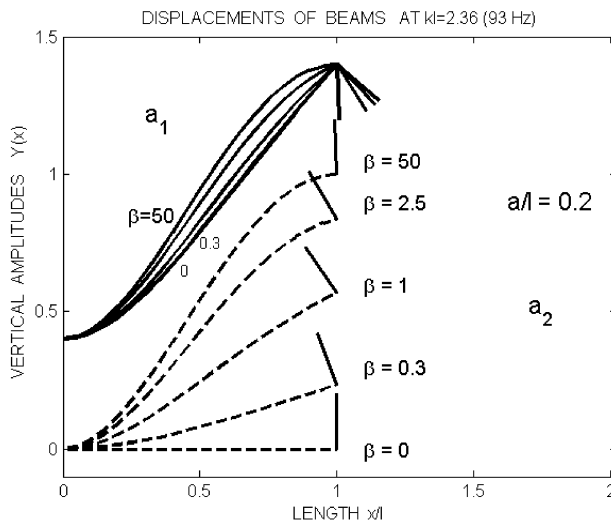

Fig.9: Variation of beams vibration modes $Y_i(x)$ with increasing dimensionless damping β at constant amplitudes $a_1/x_0 = 1$ of upper beam at $k\,l = 2.36$

6. Strength in beam roots

For reliability and durability of turbine blade disks, it is important to know the stress in the critical points of blades – particularly near the roots. In the beam model this critical point is near the fixing point at $x = 0$ and it is proportional to the curvature i.e. to the second derivative $\partial^2 y / \partial x^2$. Using equation (15) for description of stress σ in the form

$$\sigma_i = K_\mathrm{s} \max y_i''(0, t) = K_\mathrm{s}\, Y_i''(0) =$$
$$= K_\mathrm{s}^* \sqrt{\left[\tilde{S}(0)\, A_i + \tilde{T}(0)\, C_i \right]^2 + \left[\tilde{S}(0)\, B_i + \tilde{T}(0)\, D_i \right]^2}\,, \tag{22}$$

where $i = 1, 2$; K_s^* includes parameters of material and dimensions of the beam (model of blade) as it is $E\,J$, S, ρ, l etc.; A_i, B_i, C_i, D_i $(i = 1, 2)$ are constants ascertaining for given κ, ε, β from equation (17).

As seen from Fig. 8 and 9, the curvations in the beam roots increases with rising damping β. The ratio $\sigma(\beta)/\sigma(0)$ of the root stress of damped and undamped two-beams system is used for quantitative evaluation of this influence. Because the constants are canceled in this ratio and $\tilde{T}(0) = \sinh(0) + \sin(0) = 0$, the expression

$$\left(\frac{\sigma(\beta)}{\sigma(0)} \right)_i = \frac{\sqrt{A_i(\beta)^2 + B_i(\beta)^2}}{\sqrt{A_i(0)^2 + B_i(0)^2}} \tag{23}$$
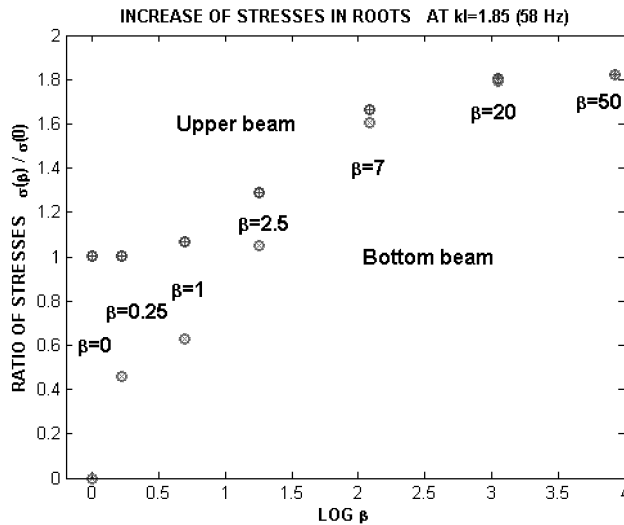
gives universal information for all similar systems.

Fig.10: Relative increase of stress $\sigma(\beta)$ in beams roots at
different damping β and at $k\,l = 1.85$ $(f = 58\,\mathrm{Hz})$

Ratio $\sigma(\beta)/\sigma(0)$ plotted versus damping parameter β in Fig. 10 shows that with increasing damping between beams, the stress near root increases and for high damping it reaches value approx. by 80 % higher than stress σ_0 at undamped cantilever beam with the same displacement on its free end. The bottom beam has zero stress at $\beta = 0$, but then $\sigma(\beta)$ rises very quickly and after $\beta > 7$ both beams have nearly the same stresses at the roots.

This diagram was calculated at $kl = 1.85$ corresponding to the first resonance peak in Fig. 7 at 58 Hz. The high resonance amplitudes appear at moderately damped systems ($\beta > 0.25$) and therefore the real stress is proportional to inverse damping value $1/\beta$ and can be calculated from cantilever theory.

Increase of stresses in beams roots in the second resonance $kl = 2.36$ (93 Hz) is evident from Fig. 11. It is similar to Fig. 10, but the most important cases for this second resonance are systems with higher damping $\beta > 7$ where the rise of $\sigma(\beta)/\sigma(0)$ is approx. 60 %.

The decrease of 60 % (Fig. 11) from 80 % in Fig. 10 is caused by stronger influence of higher modes at increasing frequency (58 Hz → 93 Hz). Let us mention that the difference of ratio $\sigma(\beta)/\sigma(0)$ for quasi-static case with very low frequency ($kl, \omega \to 0$) and at change $\beta \to 0$ to $\beta \to \infty$ is 2 that means increase of 100 %.
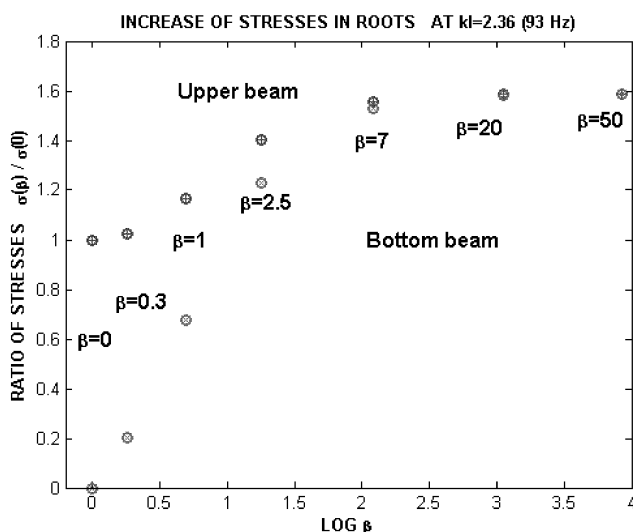

Fig.11: Relative increase of stress $\sigma(\beta)$ in beams roots at
different damping β and at $kl = 2.36$ ($f = 93$ Hz)

7. Conclusion

Forced vibrations of a system consisting of two parallel cantilever beams connected at their free ends by a viscose damping element, eccentric placed on perpendicular branches, were solved analytically and numerically.

It is shown that due to the eccentric position of contact damping area, the dynamic stiffness – force at constant displacement – and dynamic compliance – displacement at constant force – change considerably both with variable frequency of excitation and with damping. The modes of vibrations vary as well from the cantilever form to the beam form with restrained end revolution.

This variation of modes is connected also with the increase of stress in the beam root. This increase can reach up to 100 % with the damping rise from $\beta \to 0$ to $\beta \to \infty$.

Presented study was focused on system with linear viscose damping, but the gained results hold true with good approximation also for dry friction in contact area after introducing equivalent linear damping coefficient.

Acknowledgement

References

[1] Brepta R., Půst L., Turek F.: Mechanické kmitání, Sobotáles, Praha, 1994
[2] Gonda J.: Kmitanie nosníkov a hriadelov, VSAV, Bratislava, 1969
[3] Půst L.: Výpočet rámových konstrukcí ve stavbě strojů, SNTL, Praha, 1967
[4] Timoshenko S.: Vibration Problems in Engineering, Van Nostrand, New York, 1955
[5] Ziemba S.:Analiza Drgan, PWN, Warszawa 1959
[6] Chelomej V. N.: Vibracii v technike, Tom 3, Maschinostrojenie, Moskva, 1980
[7] Půst L., Veselý J., Horáček J.: Výzkum třecích účinků na modelu lopatek, Sborník konf. 'Parní turbíny a jiné turbostroje 2007', Škoda-ASI-ZČU, Plzeň, str. 19/1-10
[8] Půst L., Veselý J., Horáček J., Radolfová A.: Výzkum třecích účinků na modelu lopatek, Sborník konference 'Parní turbíny a jiné turbostroje 2008', Škoda-ASI-ZČU, Plzeň, str. 18/1–10
[9] Půst L.: Aplikovaná mechanika kontinua II, (Dynamika kontinua), Skripta ČVUT-FJFI, Praha, 1986
[10] Půst L.: Dynamic deformations of beams connected by damping element, Proc. Colloquium 'Dynamic of Machines 2009', Prague, 2009

Note: This paper is an extended version of the contribution presented at the national colloquium with international participation *Dynamics of Machines 2009* in Prague.